THE PERFORMANCE OF A DUAL-MODE POSITIONING SERVOMECHANISM WITH TIME-OPTIMAL CONTROL

A THESIS

Presented to

The Faculty of the Graduate Division

by

Rex Bartlett Simms

In Partial Fulfillment

of the Requirements for the Degree

Master of Science in Electrical Engineering

Georgia Institute of Technology

June, 1964

THE PERFORMANCE OF A DUAL-MODE POSITIONING SERVOMECHANISM WITH TIME-OPTIMAL CONTROL

Approved:

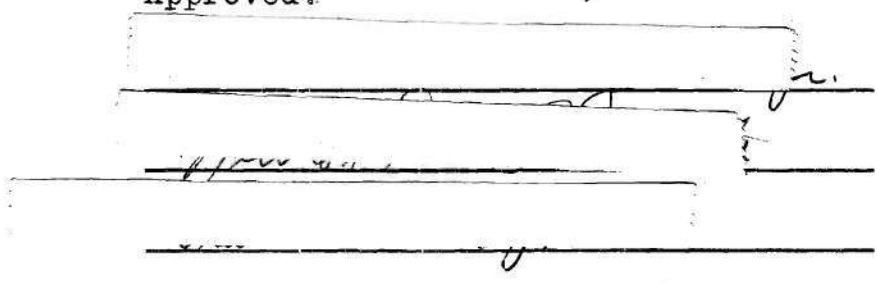

Date approved by Chairman: June 8-1964

In presenting the dissertation as a partial fulfillment of the requirements for an advanced degree from the Georgia Institute of Technology, I agree that the Library of the Institution shall make it available for inspection and circulation in accordance with its regulations governing materials of this type. I agree that permission to copy from, or to publish from, this dissertation may be granted by the professor under whose direction it was written, or, in his absence, by the dean of the Graduate Division when such copying or publication is solely for scholarly purposes and does not involve potential financial gain. It is understood that any copying from, or publication of, this dissertation which involves potential financial gain will not be allowed without written permission.

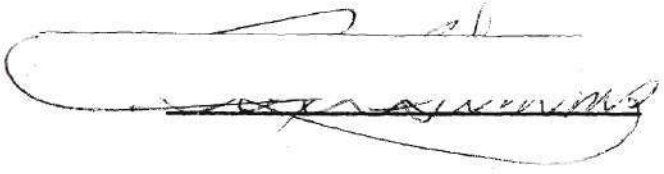

ACKNOWLEDGMENTS

The author wishes to express his sincere appreciation to Dr. F. O. Nottingham for his assistance and encouragement as thesis advisor; to Messrs. J. H. Leopold and W. B. Charter, of Zimmerman, Evans, and Leopold, Consulting Engineers, for allowing me to pursue this project while associated with the firm; to Mrs. Randy Miller who assisted in the preparation of the initial draft; to Dr. N. H. Barnette and Dr. Frank M. White, Jr., as members of the reading committee; to Dr. K. M. Murphy for advice on matters of style and format; and lastly, to my wife and children for their patience and forbearance.

TABLE OF CONTENTS

TABLE OF CONTENTS (Continued)

LIST OF TABLES

LIST OF ILLUSTRATIONS

LIST OF ILLUSTRATIONS (Continued)

SUMMARY

A positioning servomechanism having two modes of control and powered by a repulsion motor was constructed and tested. The control modes were continuous and contactor respectively.

The construction of the system was suggested by the work of Gibson and McVey (1)*. Gibson's and McVey's work describes two dual-mode systems with mode switching boundaries defined by error magnitude and the sum of error magnitude and error rate, respectively. Certain portions of these systems were simulated on an analog computer.

The system investigated by the author has a mode switching boundary defined by the sum of error magnitude and output rate. A complete system was constructed without the use of an analog computer. The error was detected by a system of synchros. The output rate was generated by a tachometer generator.

Contactor control included a time-optimal controller not present in the system of Gibson and McVey. This controller reverses the torque of the motor at the optimum time when the system is operating in the contactor mode. Optimum application of reverse torque reduces the error and

---

*Numbers in parentheses refer to the Bibliography.

output rate to zero simultaneously. The topology of the time-optimal controller was developed by simulating the phase-plane characteristics of error versus output rate, using a network synthesized from biased diodes and resistors.

The system was tested by excitation with step input displacement and variable frequency sinusoidal signals. Step input tests were performed on each mode individually and both modes combined.

The contactor mode alone, and without time-optimal control, was unstable. The addition of the continuous mode and time-optimal control to the contactor mode stabilized the system. Variable frequency tests showed that continuous mode operation was undesirably slow. The insensitivity of the electromagnetic relays of the size required suggests the use of silicon control rectifiers in this type of control system. It is entirely possible that the improved response of a system using silicon control rectifiers might not require a continuous mode. This statement is based on the assumption that silicon control rectifiers would permit the construction of a system with a smaller dead zone than permissible with electromagnetic relays.

CHAPTER I

INTRODUCTION

Statement of the Problem

The effect of time-optimal control of the contactor mode on the stability of a dual-mode, positioning servomechanism having continuous and contactor modes is studied. The theory of time-optimal ("bang-bang") position control is based on the dynamic relationship between speed and relative position in the system studied as it is slowed from full speed to rest by reversing the drive motor. In the system studied, time-optimal control is employed only when the system is operating in the contactor mode.

Positioning in minimum time is achieved for sufficiently large error by applying full voltage to the drive motor first in the desired direction and then reversing the voltage to the drive motor to achieve a braking effect. This is accomplished with the system operating in the contactor mode. The system, however, begins its positioning by operating in the continuous or small signal mode. The system must, therefore, contain a device which will switch the mode of operation from continuous mode to contactor mode.

Background

The concept of optimum step function response by a servomechanism suggests a device which will apply its maximum corrective force to any error. The contactor, or relay, is ideal for this service because it inherently possesses the characteristic of applying full available corrective force and is well suited to apply sudden reversals of the full available corrective force. The contactor, however, possesses the characteristic of limit cycling when small or no error is present and cannot follow small or arbitrary inputs accurately.

The dual-mode servomechanism, which was first suggested by McDonald (2), combines a continuous mode of operation for small signal operation, with a contactor mode of operation for errors larger than the small signal error. The contactor mode may then be optimized for the minimum time of response to a step function input of sufficient magnitude to order contactor operation. Optimization is accomplished by means of a time-optimal controller which is used to determine the optimum boundary for control reversal, sometimes referred to as a "switching line." The continuous mode is optimized for small signal inputs by inserting rate feedback. The selection of the correct mode is effected by a mode switching device which initiates switching action based on the sum of the magnitudes of error and error rate.

The approach to the design of the time-optimal

controller utilizes the phase-plane plot of the system. This is a plot of system error versus output rate. The topology of the network which combines error and output rate to produce properly timed switching action is derived from the phase-plane plot. Figure 1 shows a block diagram of the system which was investigated.

Gibson and McVey (1) have investigated a system which was partially synthesized using an analog computer. Gibson and McVey presented an analytical method for determining the stability of a dual-mode system using an extension of the describing-function method of analysis. This method has been established by the independent works of Kochenburger (3), Goldfarb (4), and Tustin (5).

This study proposes to examine the stability of a dual-mode system synthesized without the use of an analog computer. The system is powered by an alternating current repulsion motor.

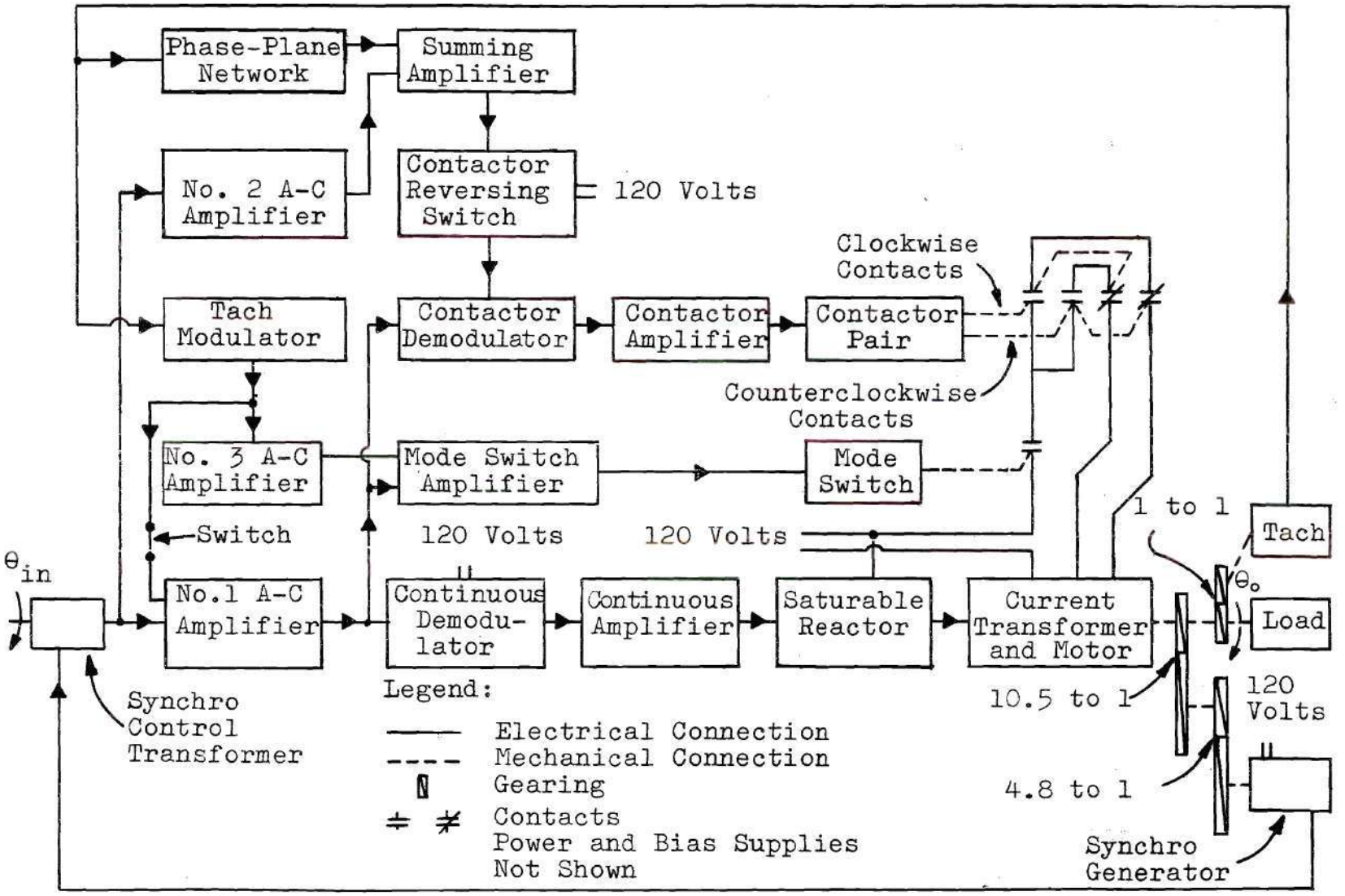

Figure 1. System Block Diagram

CHAPTER II

DESCRIPTION OF THE SYSTEM

General

By definition, a positioning servomechanism is a device which automatically corrects its output position to correspond to a new input position. This corrective action is implemented by an error signal which is described by the expression:

$$E = R-C$$

Where C is the controlled or output position

R is the reference or input position

E is the error which results from R-C.

Error Detection System

The error detection system used consists of a synchro generator and a synchro control transformer. The generator is mechanically connected to the system prime mover (source of corrective force) and electrically connected to a source of reference voltage and the control transformer. An angular difference in the position of the shafts of the control transformer and the generator results in an a-c error voltage appearing at the output terminals of the control transformer. The error detection system is shown in

Figure 2. This voltage is attenuated and then amplified by a-c amplifier No. 1 for sensitivity in the continuous and contactor modes. The error voltage is attenuated and amplified by a-c amplifier No. 2 for use in the contactor boundary switching circuitry. Diagrams of amplifiers Nos. 1 and 2 are shown in Figures 4 and 3, respectively.

The voltage output of a-c amplifier No. 1 is applied to both the continuous and contactor demodulators for conversion to direct current and application to the continuous mode and contactor mode d-c amplifiers. The output of a-c amplifier No. 1 is also applied to the mode switch amplifier. The demodulators are the sum and difference type and convert the a-c voltage which is in-phase or in reverse-phase with the reference a-c voltage to a polarity type d-c error voltage; i.e. an in-phase a-c error voltage would be demodulated as a positive d-c error voltage, and a reverse-phase a-c error voltage would be demodulated as a negative d-c error voltage. A diagram of the demodulator is shown in Figure 5.

Prime Mover

The prime mover or final control element is a repulsion motor with a modified stator winding. The stator is provided with a lap winding on which taps are brought out at 20 electrical degrees on each side of the electrical neutral of the winding as shown in Figure 6. The axis of

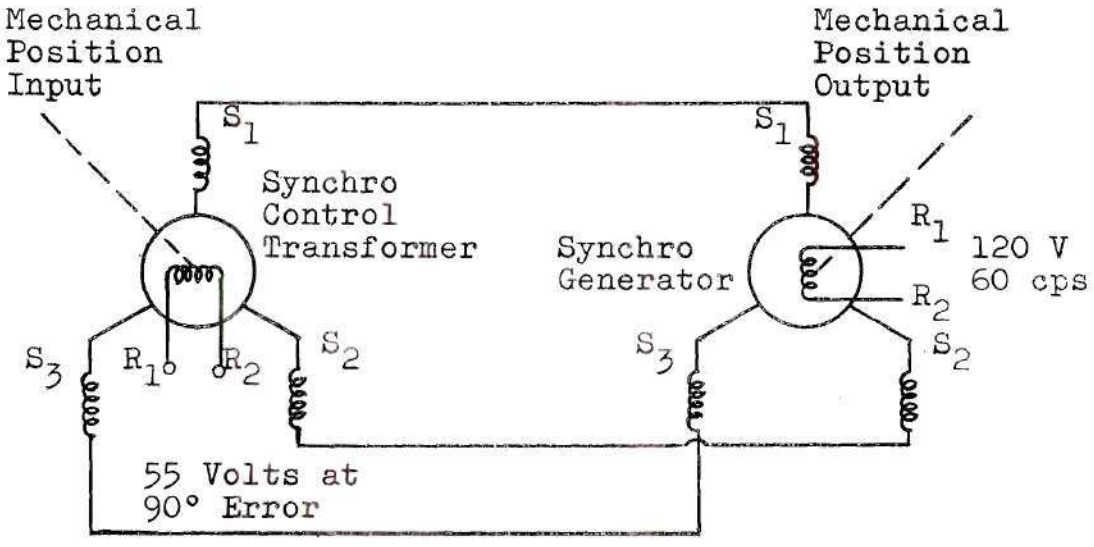

Figure 2. Error Detector

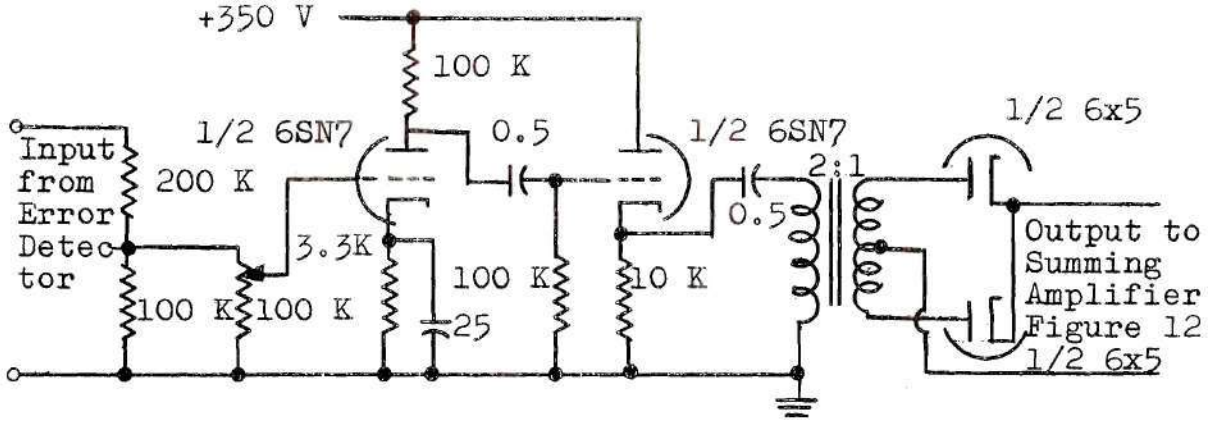

Figure 3. A-C Amplifier No. 2

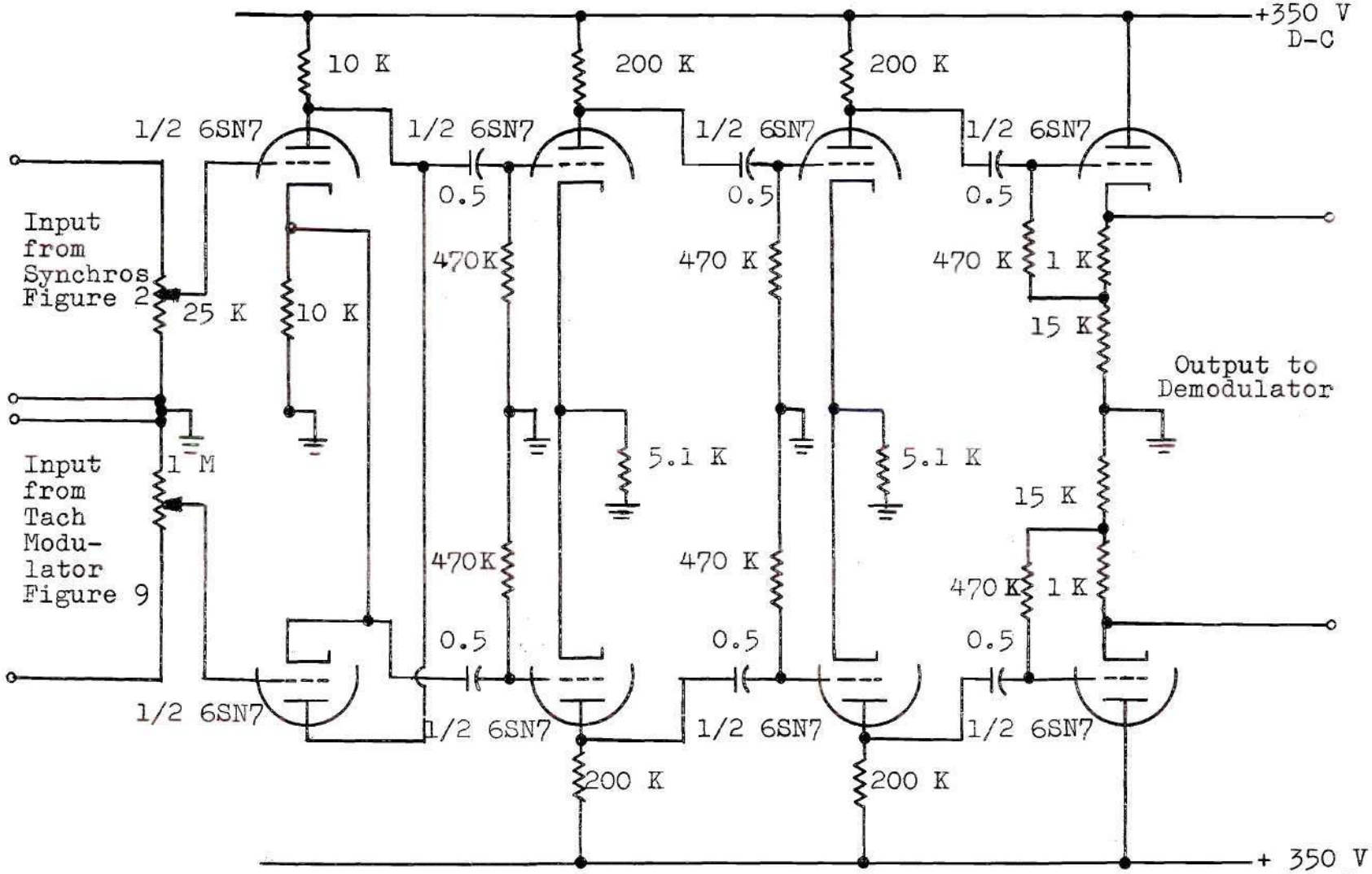

Figure 4. A-C Amplifier No. 1

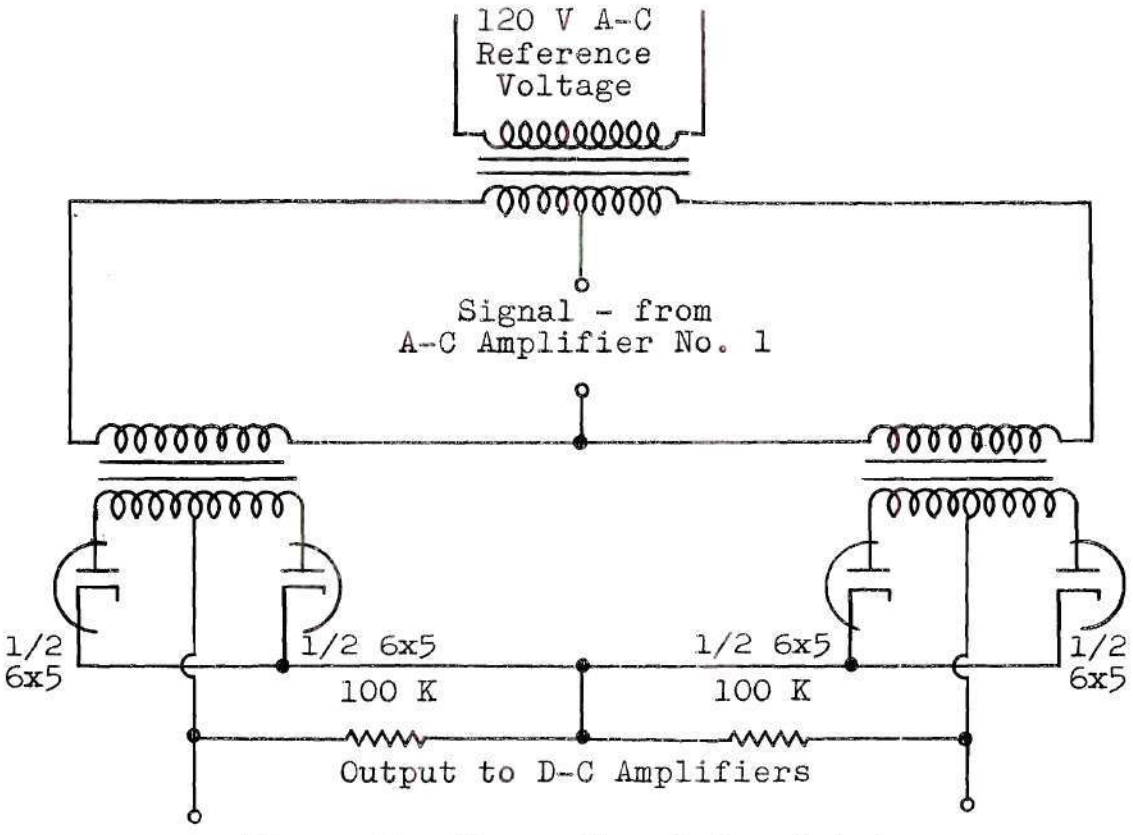

Figure 5. Error Signal Demodulator

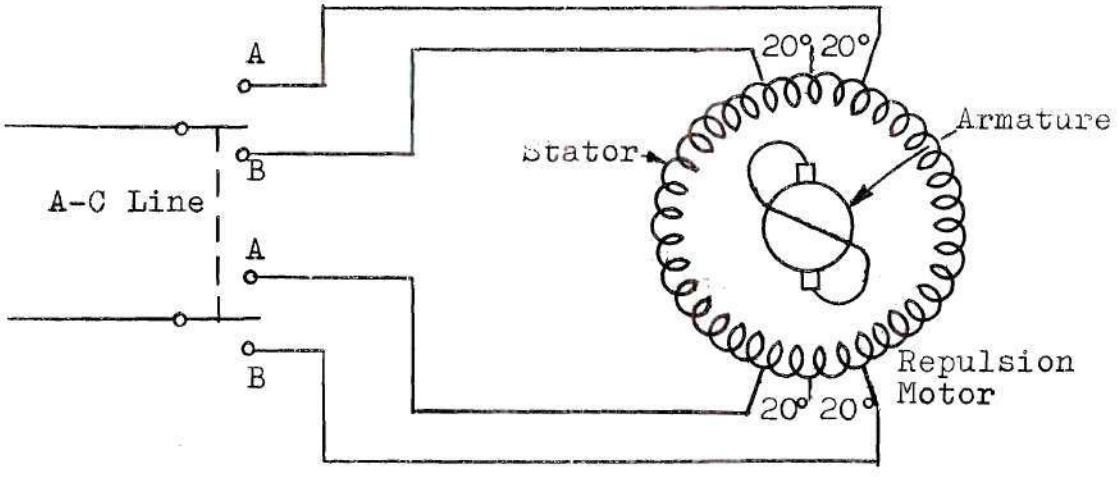

Figure 6. Basic Motor Reversing Circuit

the brushes of the repulsion motor is set in line with the electrical neutral. Therefore, if the switch is closed in position A-A, the relative stator field is displaced 20 degrees from that of the brush axis and the motor will run clockwise. If the switch is closed in position B-B, the relative position of the stator field is displaced 20 degrees counterclockwise from that of the brush axis and the motor will run counterclockwise.

In the control system designed, two electrical circuits and a special transformer replaced the double throw switch and permitted single pole double throw operation utilizing the blocking action by the transformer of current flow in the unexcited motor taps. For continuous mode operation, one of each set of taps is connected to a saturable core reactor through the special transformer. The remaining taps are connected to one side of the 120-volt line through proper transformer connections. The other side of the 120-volt line is connected to the other sides of the two saturable core reactors. The direction of rotation depends then upon which saturable core reactor is energized by the respective d-c amplifier. Under quiescent conditions, both of the reactor amplifiers are cut off. The design of the transformer is described in Appendix 1.

For contactor mode operation, the energized reactor is shunted out by the series connected contacts of the proper power contactor and the mode switch.

The load for the prime mover consists of inertia and coloumb friction. Most of this inertia is that of the motor, synchro generator and tachometer armatures with coloumb friction coming from the brushes of these devices. A flywheel was used to provide load simulation. Motor control circuitry is as shown in Figure 7.

Continuous Mode

Continuous mode control is effected by applying alternating current to the motor via two saturable core reactors, one for clockwise and one for counterclockwise rotation. The magnitude of the a-c supplied to the motor is a function of the magnitude of the error signal. The a-c is applied by varying the degree of saturation of the respective reactor with a direct current which is proportional to the error signal. This direct current is derived from the synchro error detection system by the continuous-mode demodulator. The current is amplified by bias control of a Class "B" d-c amplifier which supplies the d-c winding of each reactor. A diagram of the d-c amplifier is shown in Figure 8.

The continuous mode is stabilized by the addition of negative rate feedback which is added to the error signal via the dual input of a-c amplifier No. 1 (see Figure 4). The rate signal is produced by a d-c tachometer which is geared to the shaft of the prime mover. In order to add

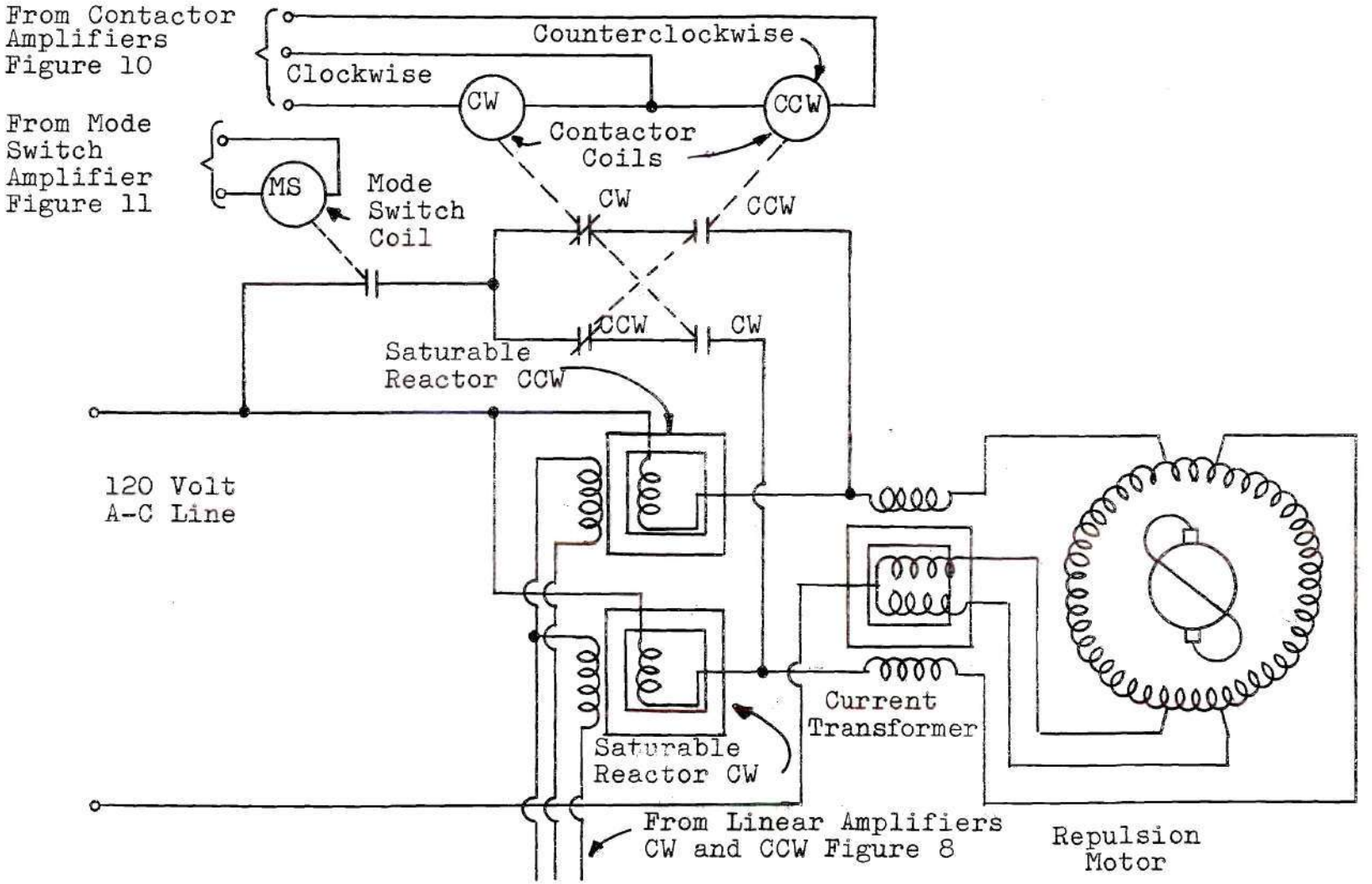

Figure 7. Motor Control Circuit

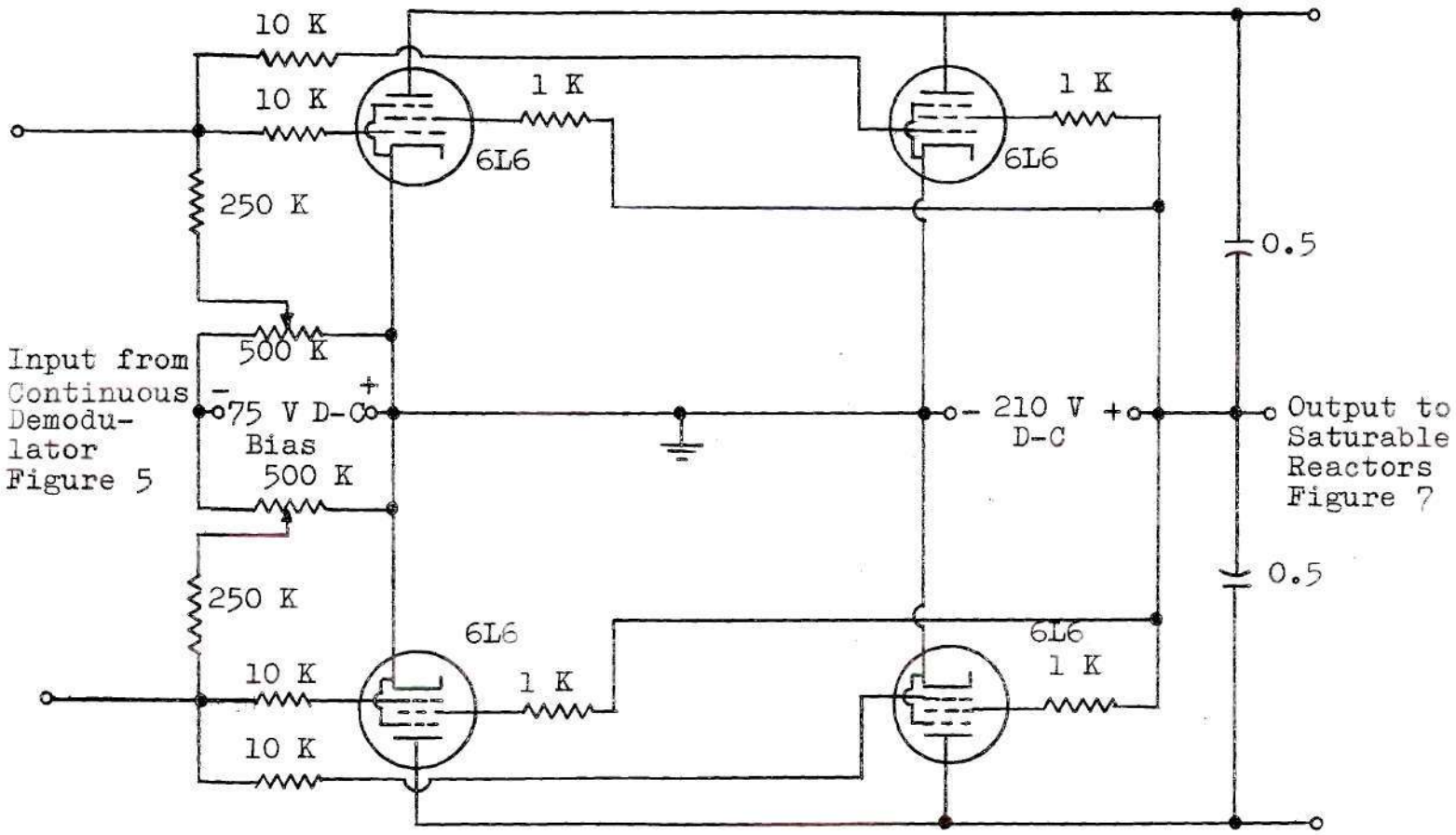

Figure 8. Continuous D-C Amplifier

this signal to the a-c error signal, the d-c signal is fed into a modulator and a resultant a-c signal is extracted. The a-c rate signal is then added to the a-c error signal at the input of No. 1 a-c amplifier. The rate feedback loop is shown in Figure 9.

Contactor Operation

Contactor operation is effected by energizing the coil of a contactor with a direct current which is derived from the error signal via the contactor demodulator and a separate bias controlled d-c amplifier. The amplifier is shown in Figure 10. A separate demodulator is used to facilitate contactor control reversal by the time-optimal circuitry. Reversal is effected by reversing the phase of the contactor demodulator reference voltage.

The contacts of each contactor are interlocked so that should both coils be energized simultaneously, no current can flow to the motor. One side of the normally open contact of each contactor is connected to a contact on the mode switch which is held open under small signal operation. The other side of the normally open contact is connected through the normally closed contact of the opposite contactor to the respective load side of the a-c winding of the saturable reactors. The remaining side of the held-open mode switch contact is connected through a manual switch to the 120-volt line. The manual switch was used to disconnect

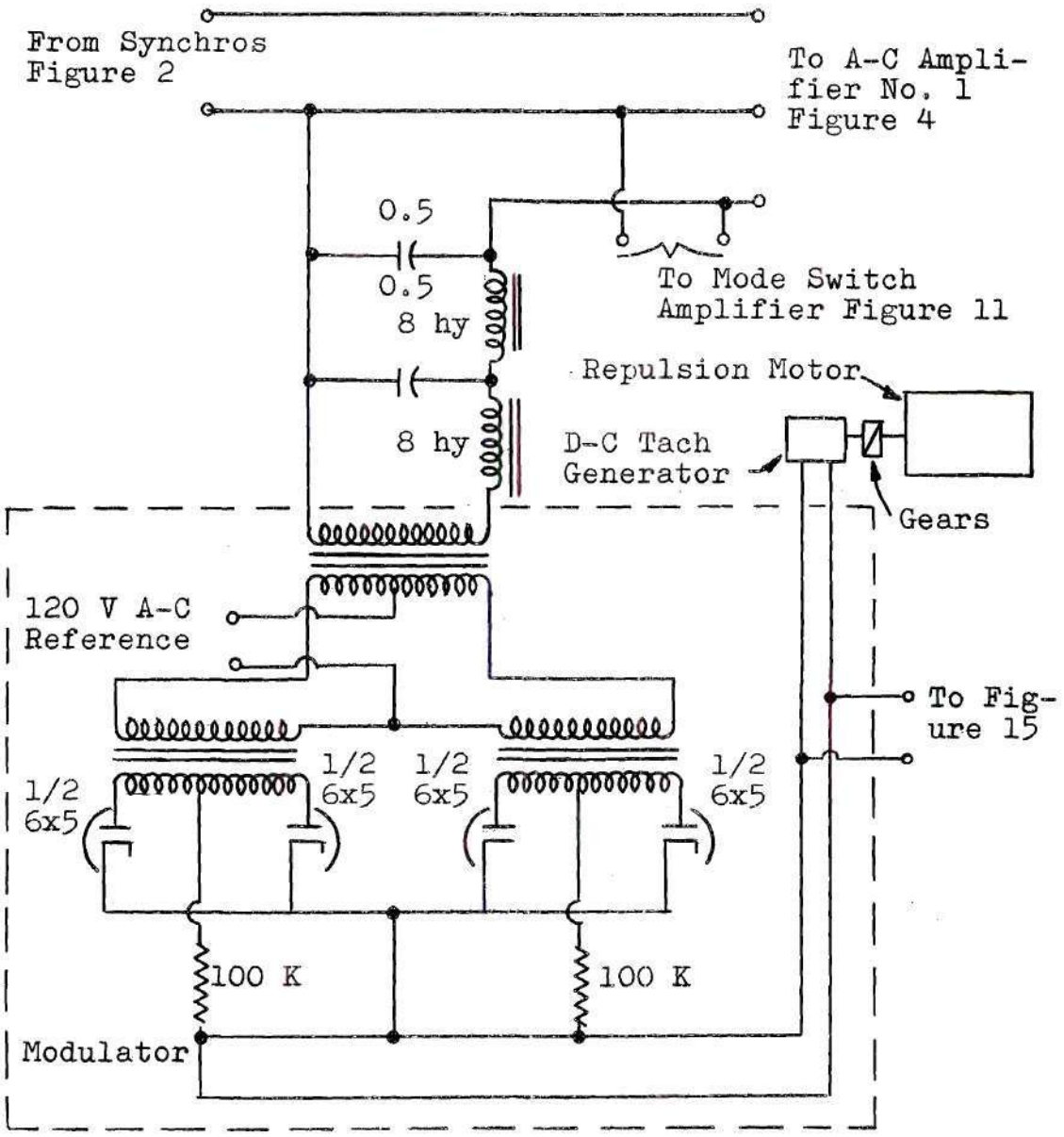

Figure 9. Rate Feedback Loop

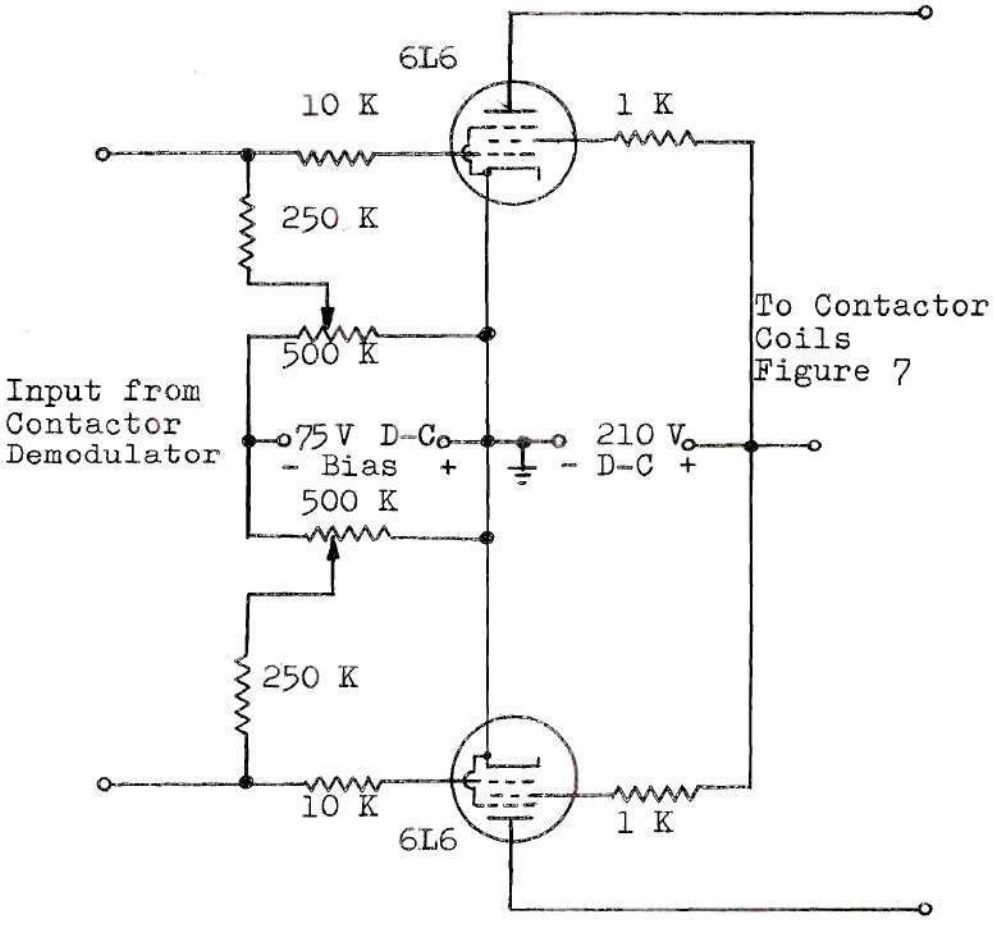

Figure 10. Contactor D-C Amplifier

the contactor mode while testing the continuous mode. Contactor control is dependent upon energization of either contactor and the mode switch, with the mode switch operating last for precise control. See Figure 7.

Mode Switch

The mode switch is operated by a d-c amplifier which is controlled by two signals which are magnitude sensitive only. One signal is derived from the error signal via a-c amplifier No. 1. The other signal is derived from the tachometer rate voltage. Both signals are rectified prior to application to the respective inputs of the mode switch amplifier. The net effect is that the mode switch is actuated by the sum of the magnitudes of the error and rate signals respectively. Mode switch and amplifier circuitry is shown in Figure 11. The rate signal is, of course, the modulated a-c signal derived from the d-c tachometer, as previously described, but amplified by a-c amplifier No. 3 for this application. The signals are attenuated at the inputs of the mode switch amplifier so as to force the mode switch operation to lag contactor operation.

Time-Optimal Switching Boundary Network

The time-optimal switching boundary network is derived from the phase-plane relationship between error and output rate as plotted on the "X-Y" recorder. The resulting curve obtained is used as the basis for the calculation of

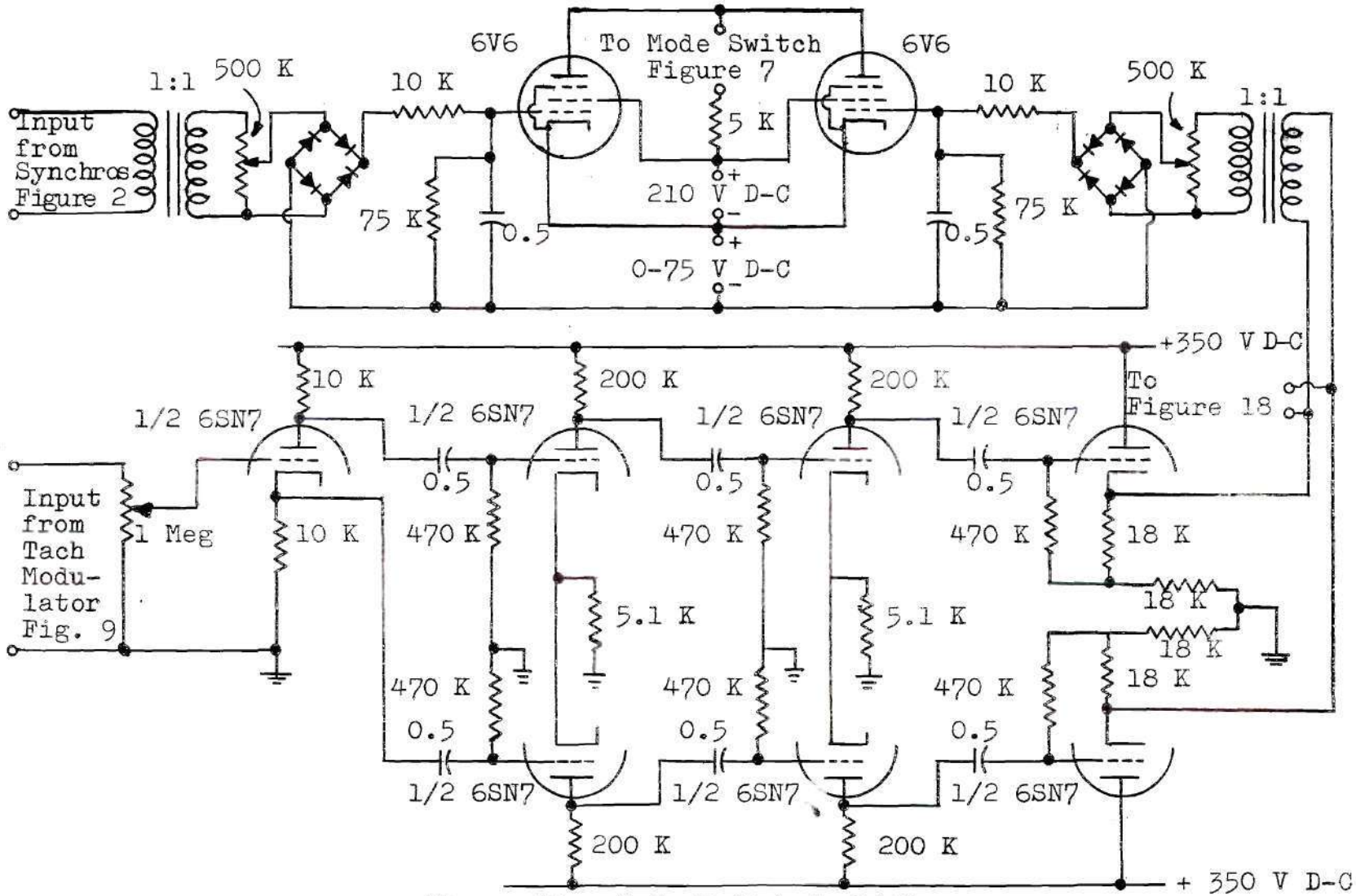

Figure 11. Mode Switch Amplifiers

elements of a biased diode network which approximates the phase-plane curve with straight line segments. The theory and design of this network is discussed in Chapter 3.

The input to the network is the d-c rate signal and the output is the simulated error signal. The synchro error signal is attenuated and amplified to the correct level by a-c amplifier No. 2 and rectified. The rectified synchro error signal and the simulated error signal are added at the input of a double cathode-follower d-c amplifier. The net result is that there is an output from the double cathode-follower when the following relationship occurs:

$$f(\dot{\theta}_o) < e$$

where $f(\dot{\theta}_o)$ is the output of the switching boundary or simulated error signal and "e" is the error signal. When $f(\dot{\theta}_o)$ is equal to "e," the output of the double cathode-follower is zero. At this instant, if the prime mover can suddenly reverse direction, "e" and $f(\dot{\theta}_o)$ should simultaneously begin to diminish at the same rate so the error and output rate should approach zero simultaneously and the system should come to rest with no position error. This relationship between "e" and $f(\dot{\theta}_o)$ permits the implementation of the critical trajectory of time-optimal ("bang-bang") control. The reversal of the prime mover is effected only when the system is operating in the contactor mode.

Reversing Switch

Reversing of the prime mover in the contactor mode is effected by reversing the phase angle of the reference voltage with respect to the a-c error voltage in the contactor demodulator. This reverses the polarity of the d-c error voltage out of the contactor demodulator and causes the energized contactor to be de-energized and the de-energized contactor to be energized. Reference voltage phase angle reversal is accomplished by using the circuitry of Figure 12. Line voltage is fed into the primary winding of an auto transformer. A resistance and a high reactance i.e., the primary of an open-circuited transformer, are connected across the secondary of the auto transformer. The reference voltage for the contactor demodulator is taken from the mid-point of the auto transformer winding and the mid-point of the series resistance-reactance combination. Phase reversal is accomplished by short circuiting the secondary of the reactance transformer with a pair of thyratrons. This effectively places the reference voltage across the other half of the auto-transformer which is 180 degrees out of phase from the voltage out when the reactance transformer's secondary is open circuited.

Firing of the thyratrons must occur before the respective contactor for either direction of error is energized for any error. This timing requirement necessitates a high gain saturating d-c amplifier which will initiate

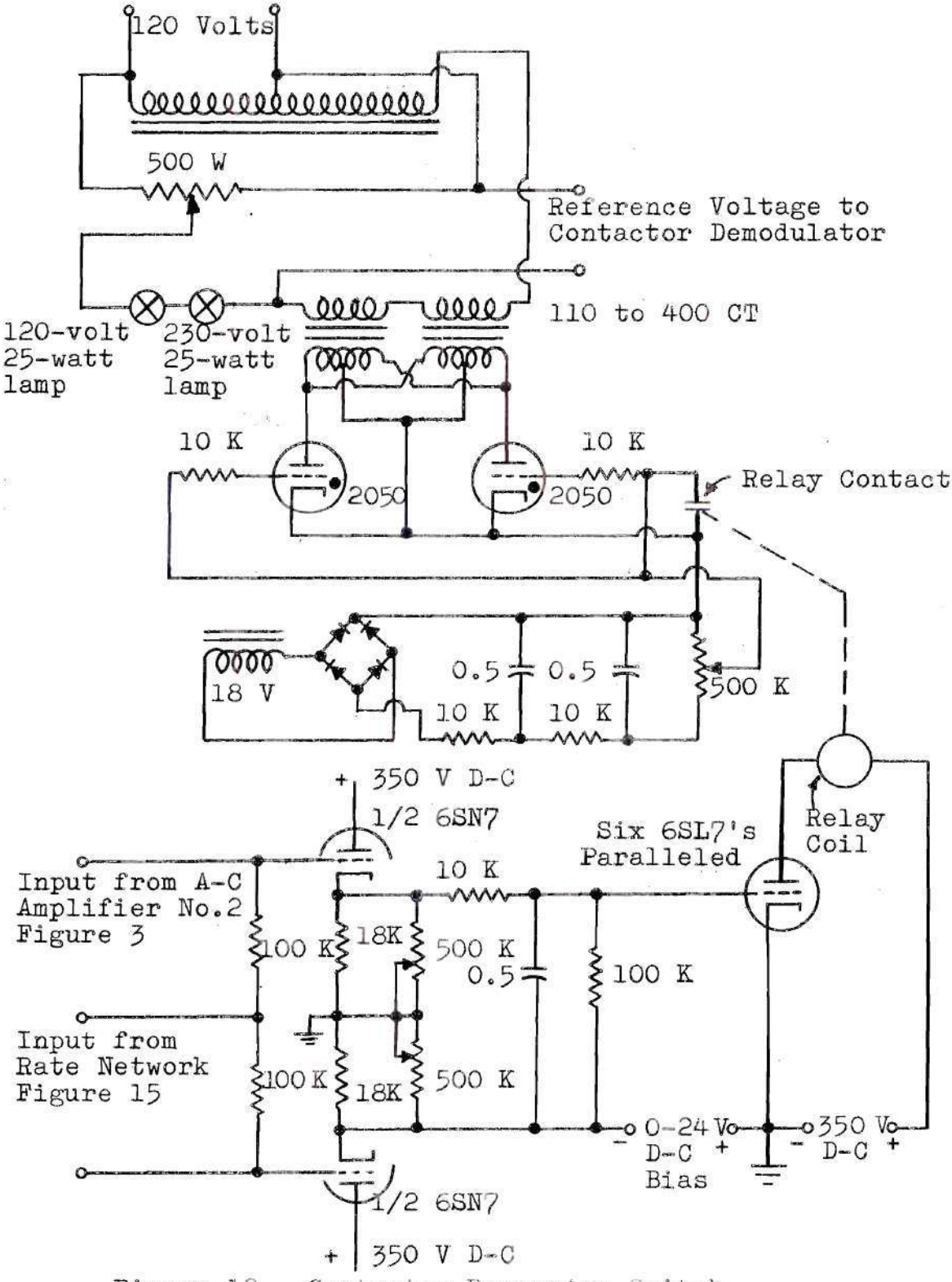

Figure 12. Contactor Reversing Switch

thyratron conduction with an extremely small output voltage from the double cathode-follower. Thyratron conduction was accomplished by construction of a d-c amplifier consisting of six 6SL7 duo-triodes connected in parallel to control a sensitive relay connected in their common plate circuits. The tubes are biased so as to turn on with the minute signal from the double cathode-follower.

The thyratrons were biased so as to be nonconducting with no signal. Operation of the relay caused a contact to close which effectively removes the thyratron bias voltage and permits the thyratrons to conduct.

CHAPTER III

DESIGN OF THE NON-LINEAR BOUNDARY SWITCHING NETWORK

General

The theory of "bang-bang" control is based on the relationship between error and error rate as the control system is decelerated at a maximum rate from full speed with simultaneous reduction of error and error rate to zero. "Bang-bang" control is effected by control reversal at the instant the magnitudes of the error and output rate become equal and the removal of correction force when both quantities reach zero simultaneously.

Network Specifications

The prerequisite for the implementation of this concept is a plot of error versus output rate under these conditions. This is known as the phase-plane plot. This plot was obtained by using an "X-Y" recorder.

The error detection system was modified to facilitate easier collection of the data. This entailed the addition of a potentiometer bridge consisting of a driven and a fixed potentiometer. The driven unit was geared to a synchro motor which was electrically driven by the synchro generator geared to the shaft of the repulsion motor. The output of this bridge and the tachometer generator were

then fed into the "X" and "Y" channels, respectively, of the "X-Y" recorder.

The "X" axis was then calibrated in degrees of motor shaft rotation. The "Y" axis was calibrated in volts. The repulsion motor is connected to a variable voltage auto-transformer and reversing switches which permit the motor to be driven at the desired speed in the desired direction directly from the a-c line. The error signal is adjusted to zero at zero speed. The motor is then energized and allowed to come up to full speed. Upon attaining full speed, the motor is reversed. Figure 13 shows the test instrumentation.

With the phase-plane curve obtained, the technique to effect "bang-bang" control consists of the design of a network which has the error rate as its input signal and a simulated error signal as its output signal as obtained from the phase-plane curve. The simulated error signal and the system error signal obtained from the synchros are then combined as shown in Figure 12 to effect control reversal.

Network Design

The design of the network follows the procedure as outlined by Fredrickson (6) and is of the biased diode type. As suggested, the network was designed to give an attenuation of 3 to 1 to conserve bias power. The network, of course, simulates the applicable portion of the phase-

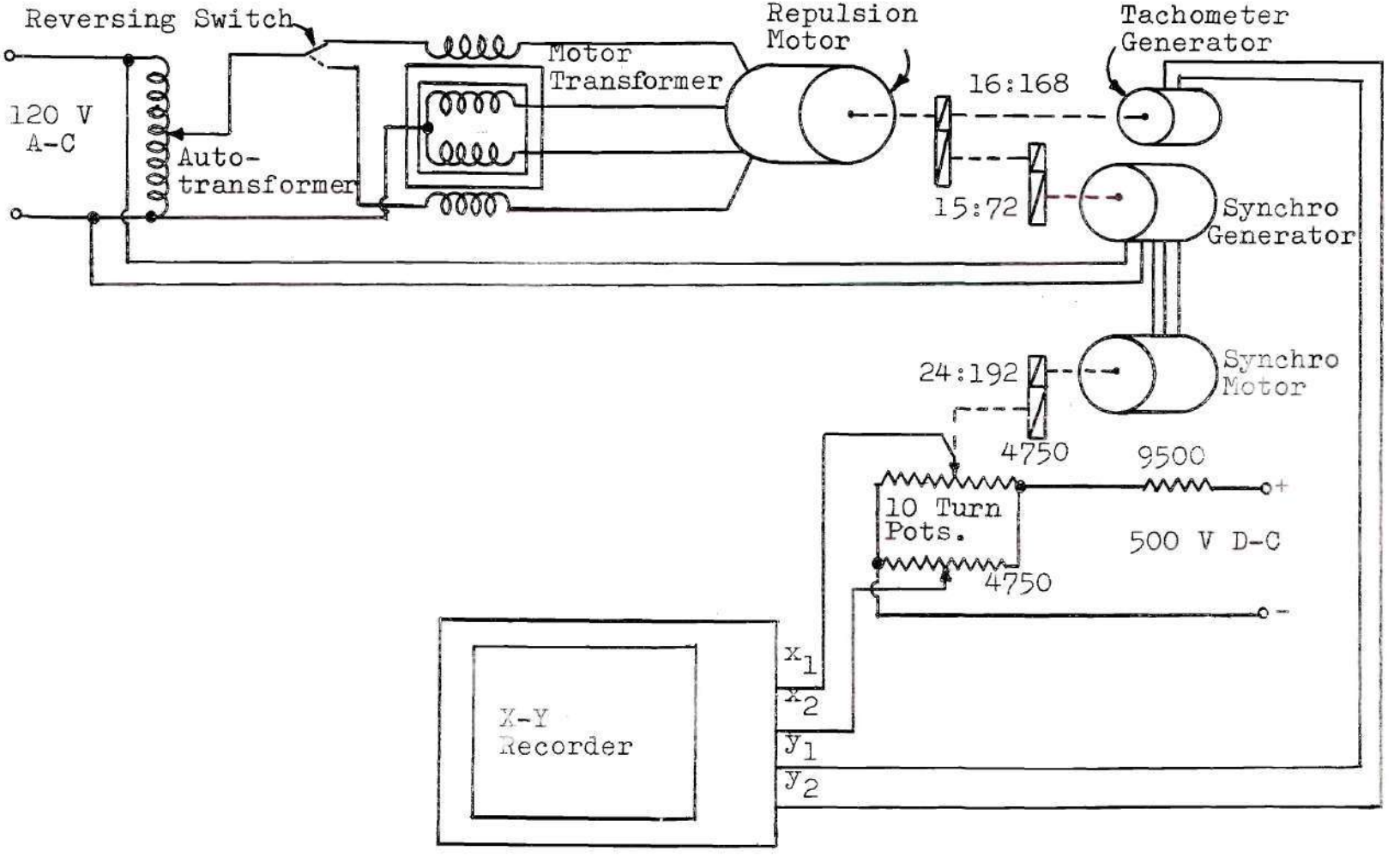

Figure 13. Instrumentation for Phase-Plane Plot

plane curve as obtained by using the "X-Y" recorder, with a number of straight line segments. A sufficient number is used to closely approximate the curve.

Seven points were chosen for the basis of calculation. The abscissa was converted from degrees of rotation of the prime mover shaft to volts output of the simulated error signal as shown in Figure 14. This necessitated the construction of an additional a-c amplifier, previously described and shown in Figure 3, to set the synchro-derived error signal at the proper magnitude for combination with the simulated error signal, $f(\dot{\theta}_o)$, to effect switching action. The network components were then calculated from the data taken from the curve as shown in Figure 14. Complete network calculations are tabulated in Appendix II. The error rate was fed into the network through a rectifier bridge to insure that the network bias would always be of the correct polarity for the polarity of the rate signal. The network is shown in Figure 15.

The network was tested by energization from the d-c tachometer with the network potentiometers set to produce the values of resistance "R_n" as computed in Appendix II. This result is superimposed on the phase-plane curve of Figure 14. Since this approximation is not optimum, it was necessary to adjust the potentiometers when testing the system to obtain optimum step function response. It is pointed out that the curve of Figure 14 is less than

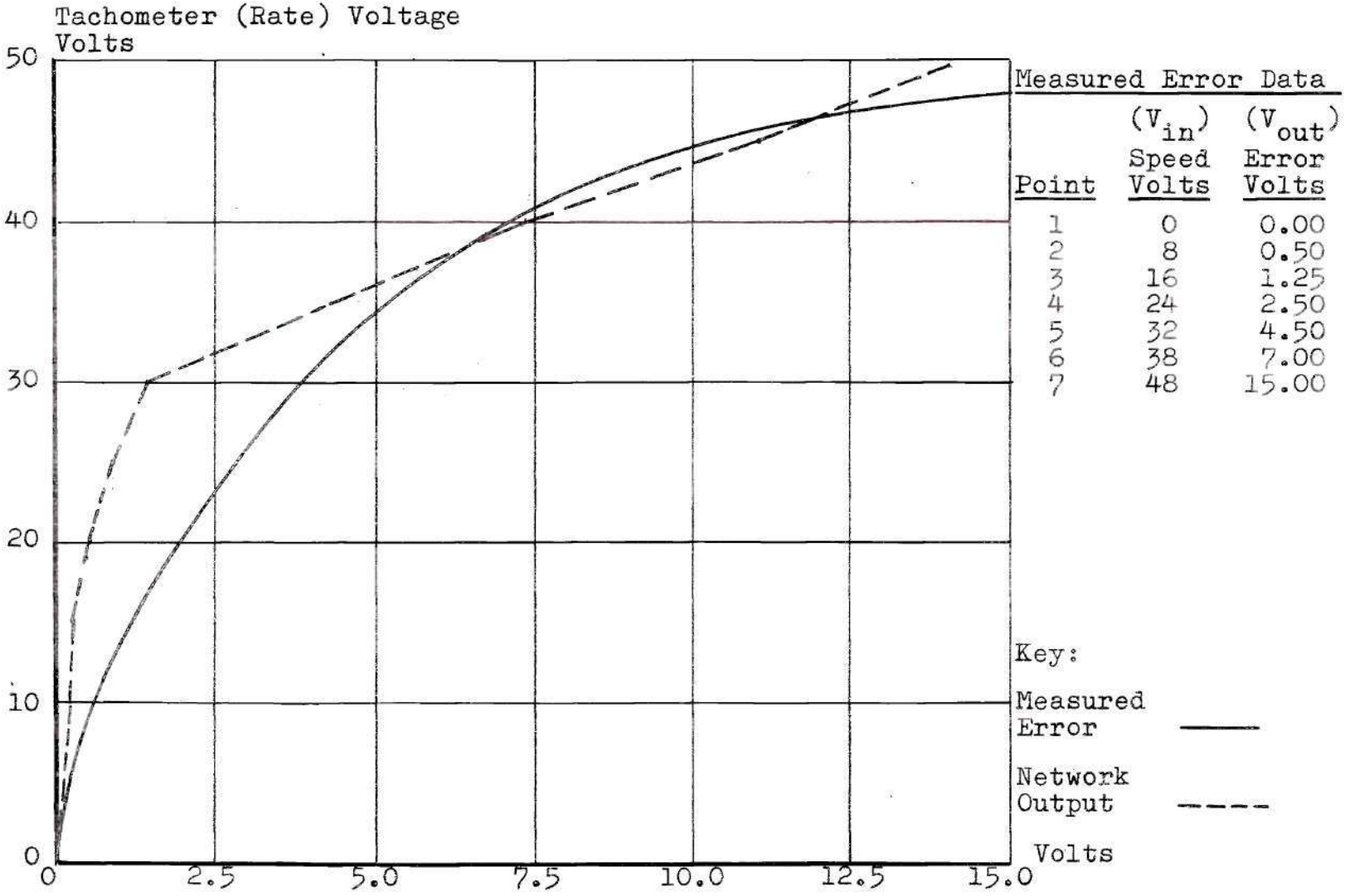

Figure 14. Phase-Plane Plot

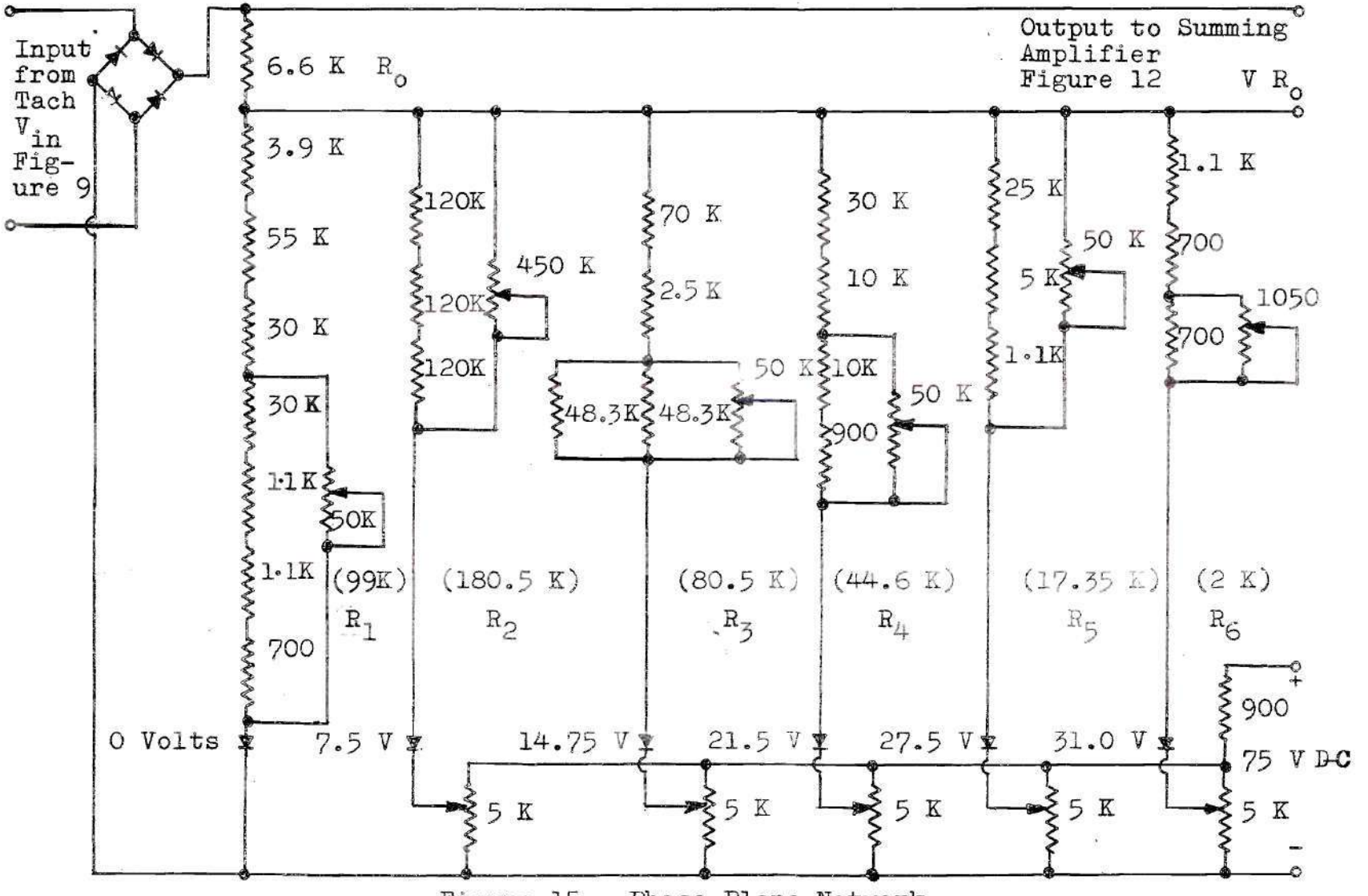

Figure 15. Phase-Plane Network

optimum because the measurement technique required includes the response time of the "X-Y" recorder.

System Photograph

A photograph of the complete system is shown in Figure 16.

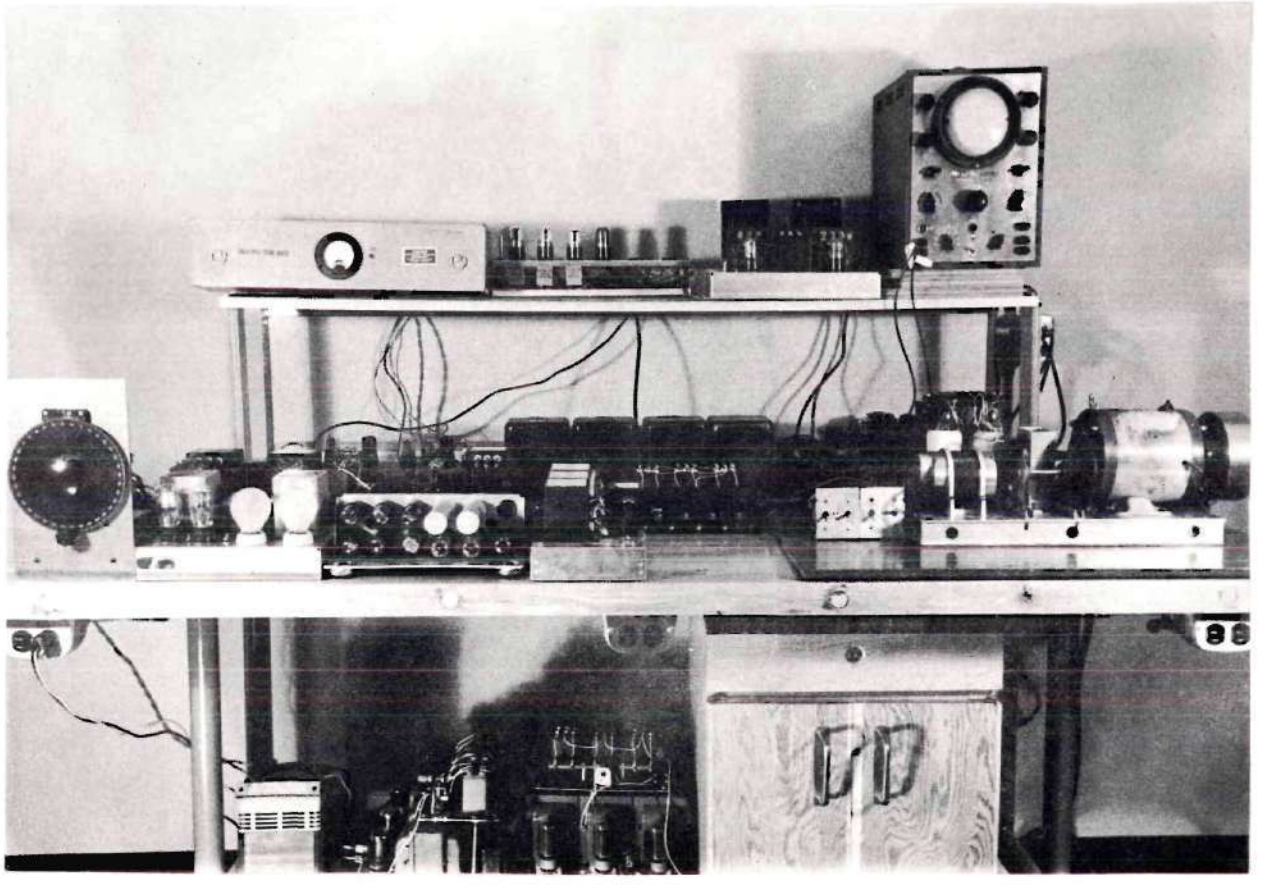

Figure 16. System Photograph

CHAPTER IV

TEST CIRCUITRY AND INSTRUMENTATION

General

With the system constructed, it was necessary to record the input and output of the system non-linearity, the mode amplifier, in order to judge the effectiveness of the time-optimal control over system response. The input to the mode amplifier consists of the sum of the magnitudes of the error signal and output rate. The output of the mode amplifier is the voltage applied to the motor during either mode of operation. The system was excited with both step and variable frequency sinusoidal signals.

The Signal Generator

The sinusoidal signal was generated by driving a synchro generator with a direct current shunt motor through suitable gear reduction. The motor field was supplied from a constant voltage supply. The motor armature was supplied from a variable-voltage regulated power supply. A direct current tachometer and an alternating current tachometer were both geared to the motor shaft. The d-c tachometer was calibrated to indicate the frequency of the signal voltage generated. Calibration was effected by the use of the a-c tachometer and an oscilloscope. Lissajous' figures

were generated on the oscilloscope with the a-c tachometer and building supply (60 cycles per second) supplied to the horizontal and vertical axes, respectively. Motor speed was adjusted until an essentially ellipsoidal figure was displayed on the oscilloscope. The ellipse represented a speed of 1800 rpm at 60 cycles per second since the tachometer is a four-pole machine. Motor speed was varied to give several frequency ratios with the d-c tachometer voltage being recorded for each frequency ratio. Calibration data is given in Appendix III. The frequency range is from 0.2 to 2.5 cycles per second. Figure 17 shows the equipment connections.

Recording Circuitry

Input and output voltages were converted to direct current to facilitate use of either the Sanborn recorder or the "X-Y" recorder. The input signals were combined, using two transformers (as shown in Figure 18) prior to rectification by a measuring demodulator. Measurement of the input voltage to the motor required the development of a switching circuit to select the voltage applied to the excited motor winding. Since the motor winding is continuous, voltage will also appear across the unexcited winding. The excited winding is the winding in which current is flowing from the motor transformer of Appendix I. The unexcited winding is the winding in which the motor current trans-

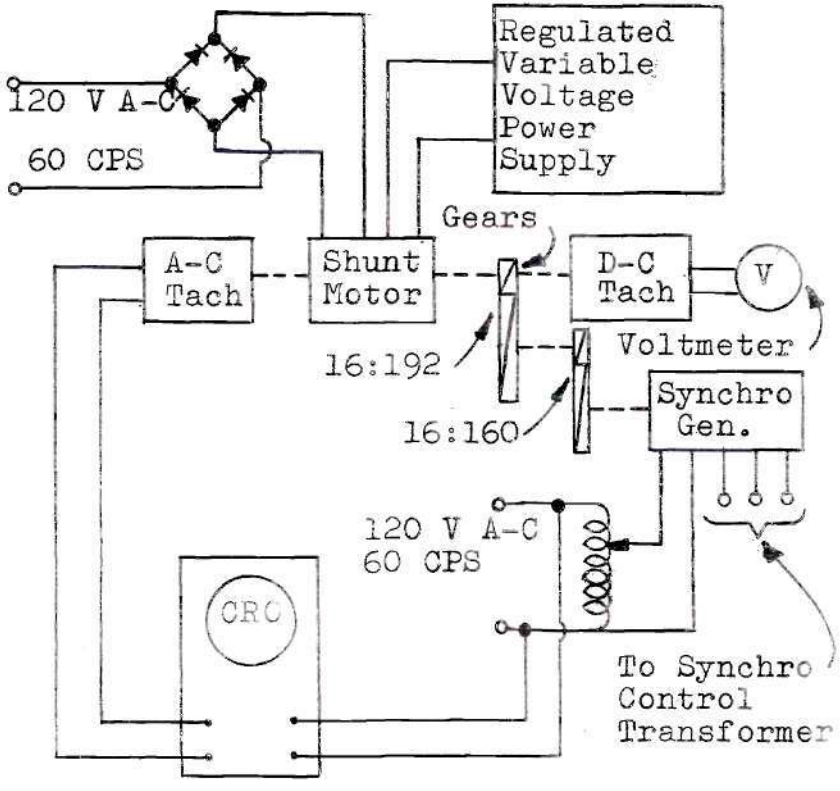

Figure 17. Calibration of Signal Generator

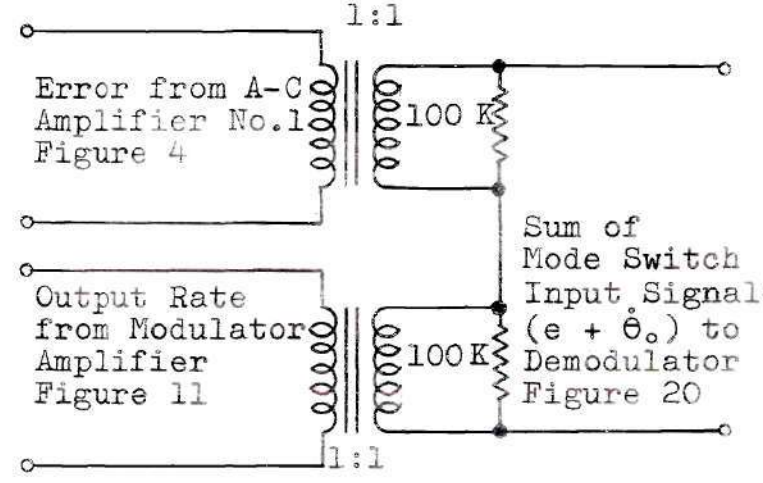

Figure 18. Signal Addition

former blocks current flow.

Separate current transformers (T20 and T30) were connected between the saturable core reactors and the motor current transformer (T10). The secondary of each transformer was loaded with a resistor and connected to a potential transformer (T21 and T31) having a single primary winding and a center-tapped secondary winding. The secondaries of T21 and T31 were connected to full-wave diode rectifiers. Each diode rectifier supplied bias control to a two-tube, duo-triode 6SL7 amplifier. The coil of a reed relay was connected in the plate circuit of each amplifier. The reed switches were connected in series with potential transformers T22 and T32, respectively. Connections were arranged so that a current flowing in the excited winding caused the reed switch to prohibit the energization of the transformer connected across the unexcited winding.

The secondaries of T22 and T32 were connected to rectifiers which were arranged to deliver a common, direct current output. Connections are as shown in Figure 19.

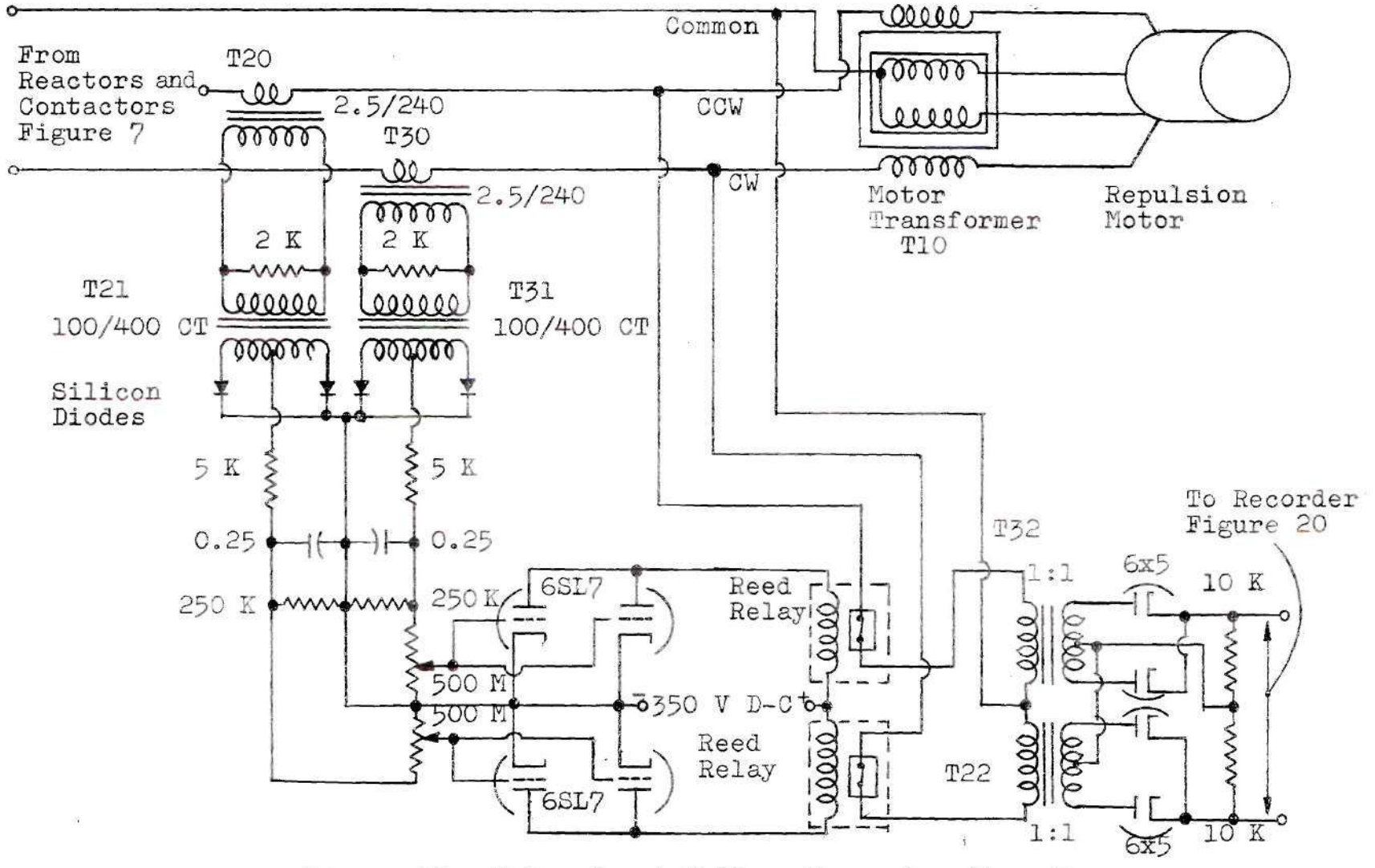

Figure 19. Motor Input Voltage Measuring Circuit

CHAPTER V

SYSTEM RESPONSE

General

The system response was investigated, using the instrumentation as described in Chapter IV. Although open loop response was desired, it was found that the system was unstable when excited sinusoidally in open loop. It was, therefore, necessary to add negative feedback. Operation showed that 50 per cent feedback was required to stabilize the system. The addition of the negative feedback permitted the introduction of both step function and variable frequency inputs without changing connections. Complete instrumentation for the system is as shown in Figure 20.

Step Function Input Data

The system was tested with the following control mode combinations:

1. Continuous only.
2. Contactor only without time-optimal control.
3. Contactor only with time-optimal control.
4. Continuous and contactor with time-optimal control.

With continuous control, the system was completely stable.

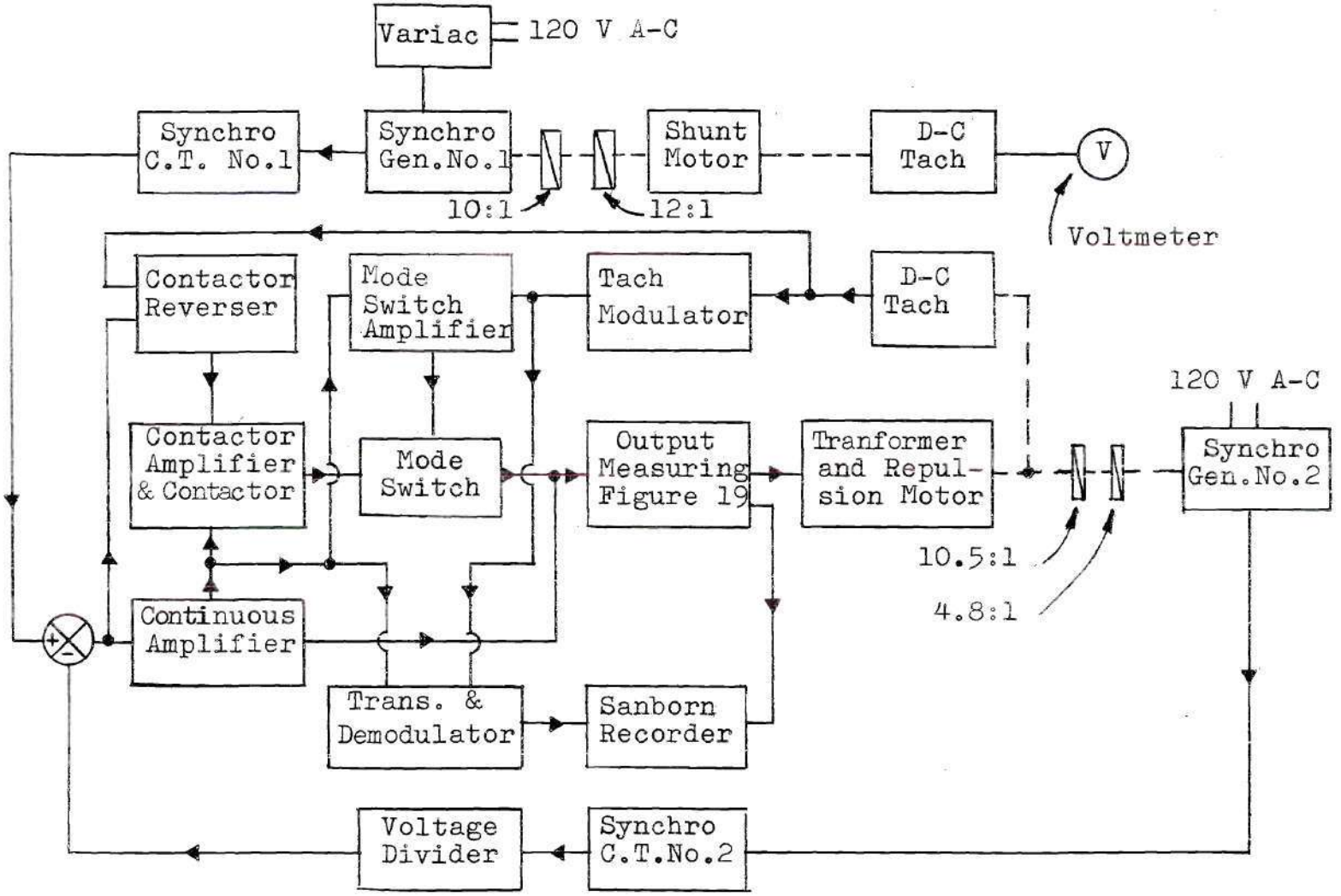

Figure 20. Test Excitation Instrumentation

With contactor control only the system hunted continuously. The addition of time-optimal control reduced the frequency of hunting. The addition of continuous control eliminated the hunting. It is to be noted that with both modes of control present, it was necessary to remove the rate feedback from the a-c amplifier No. 1, the continuous a-c amplifier. The system performed as expected with continuous control being observed for input displacements of less than five degrees and dual-mode control observed for input displacements greater than five degrees. A difference was observed between clockwise and counterclockwise positioning. This is attributable to the slight inequality between motor torques and system adjustment.

Variable Frequency Input

The system was excited with sinusoidal signals varied in the frequency range from 0.2 to 2.5 radians per second. A typical wave form for input and output is shown in Figure 21 and was obtained with an input frequency of 0.814 radians per second. The wave forms are, as expected, highly non-linear. The effect of the linear mode is most pronounced in the time interval when the contactor reversing switch has de-energized the forward contactor and has not yet energized the reverse contactor. The system seems to respond well to the time-optimal circuitry which reverses the motor with full voltage applied since no overshooting

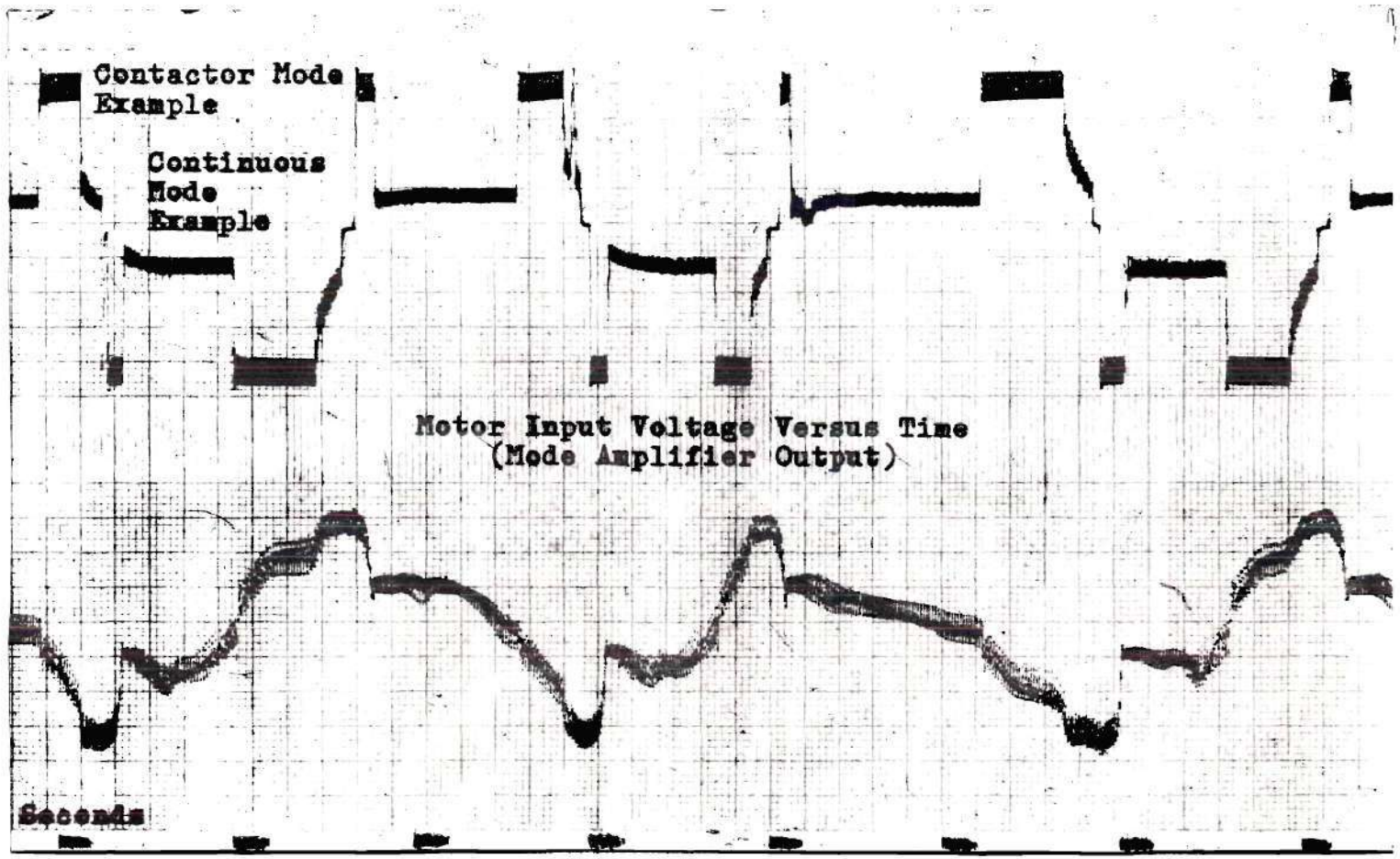

Error Plus Output Rate Versus Time (Mode Amplifier Input)
Input Frequency 0.814 Radians/Second

Figure 21. Text Excitation Recording

is indicated by the wave shape. Nonuniformity of corresponding segments of the motor input voltage wave is attributable to unequal motor torques in opposite directions of rotation and contactor hysterisis. The input range of frequencies were selected because of the frequency response of the motor when operated from the continuous mode amplifier only. The test circuitry for this data is shown in Figure 22. The gain for each frequency was determined from the slope of the plot of the "X-Y" recorder. A plot of gain versus frequency appears in Figure 23. Plotting data is tabulated in Table 1.

Stability

Figure 21 shows the system to be stable for the frequency shown, since no overshoot is present.

It was observed that the linear mode is stable with the addition of output rate feedback. The contactor mode exhibits the tendency of continuous hunting. The combination of the two modes with time-optimal control added to the contactor mode is stable. Output rate feedback is not required in the linear mode for dual-mode operation.

An analytical study of the stability of the system using the describing function method as applied by Gibson and McVey will require that the fundamental component of both input and output waveforms of Figure 21 be extracted by a Fourier analysis. This type of analysis entails a

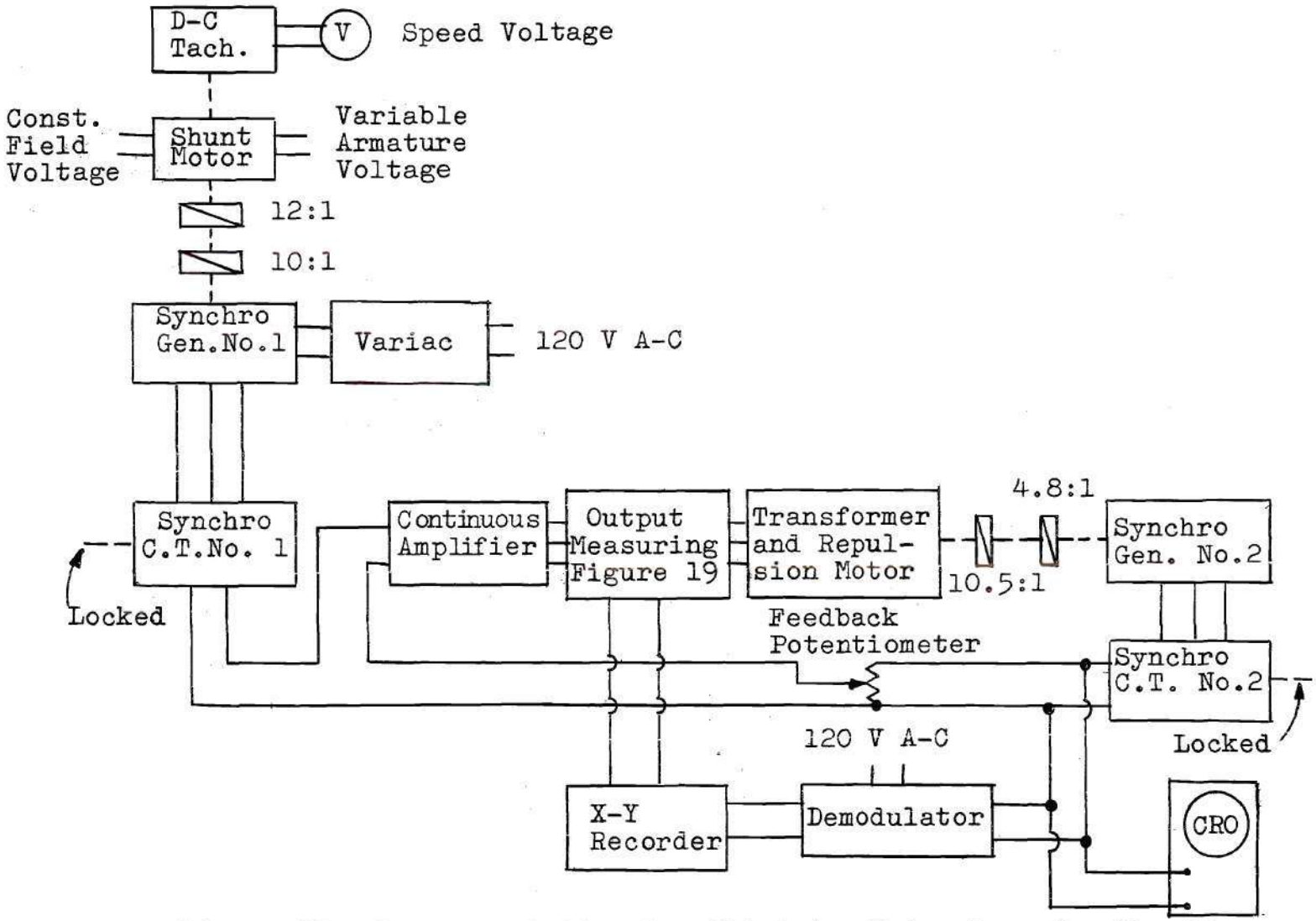

Figure 22. Instrumentation for Obtaining Motor Transfer Function

Figure 23. Motor Frequency Response Plot

Table 1. Gain Versus Frequency Data for the Frequency Response of a Repulsion Motor Controlled by a Continuous System

Input Frequency CPS	Gain Db
0.0322	7.06
0.0645	6.40
0.0807	8.75
0.0970	5.71
0.113	5.15
0.129	1.80
0.163	0.00
0.193	-2.39
0.226	-1.84
0.258	-5.65
0.290	-8.57
0.322	-11.55

thorough frequency response testing and was not included in this study.

CHAPTER VI

CONCLUSIONS AND RECOMMENDATIONS

Conclusions

Time-optimal or "bang-bang" control of the contactor mode of a dual-mode positioning servomechanism satisfactorily applies all of the available corrective torque to reduce the error of the positioning system to zero in optimum time when coupled with a continuous mode which prevents contactor limit cycling on small errors.

Examination of the test results of Figure 21 indicates that the time between contactor cycles on each half cycle of error signal is unnecessarily long. This indicates that either the continuous amplifier should have more gain or that contactor mode switching should occur earlier. Modifications would have to be made to system equipment for either possibility since the continuous mode amplifier operates at its saturation level and the mode switch and contactors are production type relays with insufficient sensitivity for operation on lower signal levels. There is also a time lag in saturable core reactor operation which delays the continuous mode.

Recommendations

The dual-mode system is necessarily complex and in-

cludes other areas for investigation not considered by this study. One area is complete frequency response testing and application of the describing function analysis. A second area could include investigation of other mode switching boundaries utilizing synthesized networks which could produce applicable functions of the error signal and its derivatives.

It is also recommended that further study be pursued on a time-optimal system which would use silicon control rectifiers in place of electromagnetic relays. The use of silicon control rectifiers could result in a system which may not require a linear mode, assuming that a system utilizing the control rectifiers will have a very small dead zone as compared to high quality electromagnetic relays.

APPENDICES

APPENDIX I

Design of Motor Current Transformer

In order to permit "three-wire control" with one wire common of the four-terminal repulsion motor, a special current transformer was designed and wound. The transformer blocks current flow through the "nonexcited" stator taps and permits reversing service with two saturable reactors in lieu of four. The transformer has four windings and was wound with two sets of concentric windings on a single window core. Individual coil design was based on 20 volts drop, with a flux density of 60,000 lines per square inch at 60 cps. The core cross-section was 1.25 inches square. Each winding was calculated to require 80 turns. Each coil was wound from 16-gage cotton-covered enameled wire.

APPENDIX II

Calculation of the Phase-Plane Network

Refer to Figure 15. V_{in} is supplied from a d-c permanent magnet tachometer-generator which has a resistance of 1,000 ohms. The tachometer also feeds a modulator with 20,000 ohms input resistance. Assume that the tachometer should not be loaded with an impedance of less than 10,00 ohms. The network must, therefore, have an input resistance of 20,000 ohms. Also, assume maximum tachometer voltage to be 48 volts. Then,

$$I_{in} = \frac{48}{20,000} = 2.4 \text{ milliamperes}$$

$$V_{R_o} = V_{out}$$

Assume

$$V_{out} = 15 \text{ volts}$$

$$R_o = \frac{15}{2.4 \times 10^{-3}} = 6,600 \text{ ohms}$$

Use

$$R_o = 6,600 \text{ ohms}.$$

APPENDIX II (Continued)

The bias voltages are calculated from values taken from the curve of Figure 14, using the equation:

$$V_{B_n} = V_{in_n} - V_{out_n}$$

Where V_{B_n} is the bias voltage for point "n," V_{in_n} is the input voltage (speed voltage) for point "n"; V_{out_n} is the output voltage (simulated error) for point "n"; "n" is a point on the curve of Figure 14.

The values selected must satisfy the condition:

$$V_{B_n} < V_{B_{n+1}}$$

Next, the parallel resistors, R_n, were calculated from the equation:

$$R_n = \frac{A_n R_o}{C_n - \sum_{j=1}^{n-1} B_j}$$

Where

$$A_n = V_{in'} - V_{out'} - B_{B_n}$$

$$C_n = V_{out'}$$

$$B_j = V_{in'} - V_{out'} - V_{B_j} = V_{B_{n-1}} - V_{B_j}$$

APPENDIX II (Continued)

The calculations were simplified by performing the operation in the format as shown in Table 2. The primes (') denote (n+1). Finally, the values of R_n computed are adjusted to standard values of resistance. The series parallel network of Figure 24 permits sensitive adjustment of standard resistors to a particular value, R_t, when the following relationships hold:

$$\text{Case I} - \quad 20\ R_t > R_z > 2\ R_t$$

$$R_x = 0$$

$$R_y = \frac{1.1\ R_t\ R_z}{R_z - 1.1\ R_t}$$

$$\text{Case II} - \quad 1/3\ R_t < R_z < 2\ R_t$$

$$R_x = \frac{0.9\ R_t\ R_z}{R_z - 0.2\ R_t}$$

R_z was selected and R_x and R_y calculated. The nearest 5 per cent standard resistor was used with:

$$R_y \text{ std} > R_y \text{ calc.} \text{ and } R_x \text{ std} \leqq R_x \text{ calc.}$$

Table 2. Calculation of the Parallel Resistors "R_n" for the Phase-Plane Network

OPERATION	R_1	R_2	R_3	R_4	R_5	R_6
$V_{in} - V_{out}$	7.50	14.75	21.50	27.50	31.00	33.00
V_{B_n}	0	7.50	14.75	21.50	27.50	31.00
A_n	7.50	7.25	6.75	6.00	3.50	2.00
V_{B_1}		0	0	0	0	0
V_{B_2}			7.50	7.50	7.50	7.50
V_{B_3}				14.75	14.75	14.75
V_{B_4}					21.50	21.50
V_{B_5}						27.50
$V_{B_{n+1}} - V_{B_1}$		14.75	21.50	27.50	31.00	33.00
$R_o * R_1$		0.0667	0.0667	0.0667	0.0667	0.0667
B_1		0.985	1.435	1.835	2.07	2.20
$V_{B_{n+1}} - V_{B_2}$			14.00	20.00	23.50	25.50
$R_o * R_2$			0.0366	0.0366	0.0366	0.0366
B_2			0.512	0.732	0.860	0.934

Table 2. Calculation of the Parallel Resistors "R_n" for the Phase-Plane Network (Continued)

OPERATION	R_1	R_2	R_3	R_4	R_5	R_6
$V_{B_{n+1}} - V_{B_3}$				12.75	16.25	18.25
$R_o \div R_3$				0.082	0.082	0.082
B_3				1.045	1.331	1.495
$V_{B_{n+1}} - V_{B_4}$					9.50	11.50
$R_o \div R_4$					0.148	0.148
B_4					1.405	1.70
$V_{B_{n+1}} - V_{B_5}$						5.50
$R_o \div R_5$						0.38
B_5						2.09
$V_{out'}$	0.50	1.250	2.500	4.500	7.00	15.00
B_n	0.00	0.985	1.947	3.612	5.67	8.419
$V_{out'} - \sum B$	0.50	0.265	0.553	0.888	1.33	6.581
$R_n = \frac{A_n R_o}{V_{out'} - \sum B}$	99,000	180,500	80,500	44,600	17,350	2,000

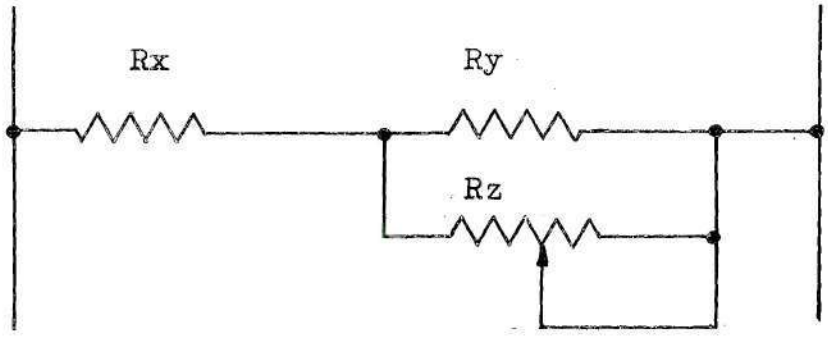

Figure 24. "R_n" Network

APPENDIX III

Calibration of Signal Generator

Data: A tabulation of the calibration data for the signal generator described in Chapter IV is presented in Table 3.

Table 3. Calibration of Signal Generator

Lissajous' Figure Ratio	Tachometer Speeds	D-C Tach Voltage	D-C Tach Volts/1000 RPM
1 : 3	600	13.0	21.5
1 : 2	900	19.2	21.3
2 : 3	1200	29.1	23.3
1 : 1	1800	38.5	21.3
3 : 2	2700	57.9	19.3
2 : 1	3600	75.5	21.0
5 : 2	4500	99.0	22.0

Average D-C tachometer voltage per 1000 RPM = 21.4 = K

Calculation: The synchro generator frequency constant per volt of d-c tachometer output was calculated as follows:

W_k = frequency of synchro generator output in radius per second.

K = d-c tachometer voltage constant = 21.4 volts per 1000 rpm.

N = gear ratio between d-c tachometer shaft and synchro generator shaft

$= \frac{192}{16} \times \frac{160}{16} = 120$ from Figure 17.

W_k = frequency constant in units of radians/volt second.

APPENDIX III (Continued)

$$W_k = \frac{2\pi}{60\ KN} = \frac{2\pi(1000)}{(60)(21.4)(120)} = 0.0404\ \frac{\text{radian}}{\text{volt-second}}$$

f_k = frequency constant in units of cycles per second

$$= \frac{1}{60\ KN} = 0.00644\ \frac{\text{cycles}}{\text{volt-second}}$$

BIBLIOGRAPHY

BIBLIOGRAPHY

1. Gibson, J. E., and McVey, E. S. "Stability Analysis of Dual-Mode Servomechanisms" American Institute of Electrical Engineers Transactions, Vol. 49, Part 2, July 1960, pp. 173-179.

2. McDonald, D. "Multiple Mode Operation of Servomechanisms" Review of Scientific Instruments, New York, New York, Vol. 23, 1952, pp. 22-30.

3. Kochenburger, R. J. "A Frequency Response Method for Analyzing and Synthesizing Contactor Servomechanisms" American Institute of Electrical Engineers Transactions, Vol. 69, Part 1, 1950, pp. 270-83.

4. Goldfarb, L. C. "On Some Nonlinear Phenomena in Regulatory Systems" Automatika Telemekhanika, Moscow, USSR, Vol. 8, No. 5, Sept. - Oct. 1947, pp. 375-83.

5. Tustin, A. "The Effects of Backlash and of Speed Development Friction on the Stability of Closed Cycle Control Systems" Institution of Electrical Engineers, London, England, Vol. 94, Part II-A, No. 1, 1947.

6. Fredricksen, R. T. "A Way to Design Low-Loss Nonlinear Networks" Control Engineering, Vol. 9, June, 1962.